Acute hydroxyurea-induced replication blockade results in replisome components disengagement from nascent DNA without causing fork collapse

Amaia Ercilla[1], Sonia Feu[1], Sergi Aranda[2], Alba Llopis[1], Sólveig Hlín Brynjólfsdóttir[3], Claus Storgaard Sørensen[3], Luis Ignacio Toledo[4] and Neus Agell[1*]

[1] Departament de Biomedicina, Facultat de Medicina, Universitat de Barcelona, Institut d'Investigacions Biomèdiques August Pi i Sunyer (IDIBAPS), Barcelona, 08036, Spain

[2] Centre for Genomic Regulation (CRG), The Barcelona Institute of Science and Technology, Barcelona, 08003, Spain

[3] Biotech Research and Innovation Centre (BRIC), University of Copenhagen, Copenhagen, DK-2200, Denmark

[4] Centre for Chromosome Stability (CCS), University of Copenhagen, Copenhagen, DK-2200, Denmark

* Corresponding author and lead contact: neusagell@ub.edu

Present Address: Amaia Ercilla, Centre for Chromosome Stability (CCS), University of Copenhagen, Copenhagen, DK-2200, Denmark

Neus Agell ORCID: 0000-0002-1205-6074

Amaia Ercilla ORCID: 0000-0001-8999-7131

Abstract

During S phase, replication forks can encounter several obstacles that lead to fork stalling, which if persistent might result in fork collapse. To avoid this collapse and to preserve the competence to restart, cells have developed mechanisms that maintain fork stability upon replication stress. In this study, we aimed to understand the mechanisms involved in fork stability maintenance in non-transformed human cells by performing an iPOND-MS analysis in hTERT-RPE cells under different replication stress conditions. Our results show that acute hydroxyurea-induced replication blockade causes the accumulation of large amounts of ssDNA at the fork. Remarkably, this results in the disengagement of replisome components from nascent DNA without compromising fork restart. Notably, CMG helicase maintains its integrity and replisome components remain associated with chromatin upon acute hydroxyurea treatment, whereas replisome stability is lost upon a sustained replication stress that compromises the competence to restart.

Keywords

iPOND, replication fork stability, CMG, replication stress

Abbreviations

CMG: Cdc45-MCM-GINS
DSBs: double strand breaks
HR: homologous recombination
BIR: break-induced replication
ssDNA: single-stranded DNA
HU: hydroxyurea
FBS: fetal bovine serum
PFA: paraformaldehyde
RT: room temperature
PIC: protease inhibitor cocktail
PI: propidium iodide
iPOND: isolation of proteins on nascent DNA
MS: mass spectrometry
WB: western blot
QIBC: quantitative image-based cytometry
RPC: Replication Pausing Complex

Introduction

Several endogenous and exogenous factors can compromise DNA replication dynamics, thereby resulting in the accumulation of replication stress, one of the major sources of genomic instability. Cells respond to this stress by activating several mechanisms to ensure the stabilization of forks, prevent origin firing and cell cycle progression, and, thus, avoid cell division in the presence of under-replicated or damaged DNA [1]. However, extensive replication stress can result in the loss of fork stability and therefore fork collapse [2].

Fork collapse has been used to describe several potentially different processes, including replisome dissociation (loss of replisome stability) and the formation of double strand breaks (DSBs). Therefore, fork collapse has usually been understood as a pathological process involving the inactivation of replication forks [2, 3]. Moreover, despite the fact that evidence relating to the possible reactivation of collapsed forks has increased in recent years, this reactivation might be mediated by a sub-type of homologous recombination (HR) known as break-induced replication (BIR) which is highly mutagenic [4], thus indicating that the prevention of fork collapse is essential to preserve genome stability.

In response to fork stalling or slowdown, the single-stranded DNA (ssDNA) that accumulates at stalled forks is protected by the heterotrimeric complex RPA. This RPA-coated ssDNA acts as a platform for the recruitment of ATR kinase [5], among other proteins. Once activated, ATR and its downstream kinase Chk1 [6] are believed to maintain the stability of the fork through several mechanisms. For instance, ATR-mediated origin firing inhibition prevents the extensive ssDNA accumulation, which results in RPA exhaustion and global replication fork breakage [7]. Moreover, ATR promotes the association of FANCD2 with MCM helicase to restrain fork progression and prevent ssDNA accumulation [8]. Furthermore, Chk1 protects replication forks from Mus81 endonuclease-mediated fork breakage [9]. Additionally, chromatin immunoprecipitation studies on yeast concluded that replisome is disassembled in the absence of checkpoint kinases after exposure to hydroxyurea (HU), thus indicating a possible role for ATR in replisome stabilization [10–12]. However, this idea has been challenged by other studies [13, 14], so the maintenance of replisome stability during replication stress and the role of ATR in this process remain controversial.

Proteins other than RPA are also involved in ssDNA and replication fork protection. For example, cohesins are thought to participate in fork protection and stability maintenance [15, 16]. Additionally, Rad51 protects ssDNA from Mre11 nuclease-mediated degradation [17]. Moreover, BRCA2 and FANCD2, among others, contribute to ssDNA protection in a Rad51-dependent manner [18–20]. In addition to its role in protecting ssDNA, Rad51 is also involved in HR-independent fork restart [2] and the promotion of fork reversal [21, 22].

According to our previous data, the competence to restart is maintained in non-transformed human cells after acute but not sustained HU treatment [23]. To gain a better understanding of the mechanisms involved in fork stability maintenance in non-transformed human cells, we analyzed the HU-induced changes at replication fork level in hTERT-RPE cells under those conditions. Our data show that acute HU-induced replication blockade generates the accumulation of large amounts of ssDNA at parental DNA strand. Strikingly, in contrast to findings in other models [14], our iPOND data show that replisome components are disengaged from nascent DNA under these conditions in non-transformed human hTERT-RPE cells. Interestingly, replisome stability is maintained and forks preserve the ability to restart upon acute HU treatment despite this disengagement. By contrast, sustained replication blockade results in the dissociation of the replisome components and fork collapse.

Materials and Methods

Cell culture, synchronization and drugs

hTERT-RPE cells were grown in DMEM: Ham's F12 (1:1, Biological Industries) medium supplemented with 6% fetal bovine serum (FBS, Biological Industries), 1% non-essential amino acids (Biological Industries), 2 mM L-glutamine (Sigma-Aldrich), 1 mM pyruvic acid (Sigma-Aldrich), 50 U/mL penicillin and 50 µg/mL streptomycin (Biological Industries).

For S-phase synchronization, cells were cultured in thymidine-containing medium for 22 h, washed with PBS and released into fresh medium for 2 h.

Drugs were used as follows, unless otherwise specified: 10 µM BrdU (Sigma-Aldrich), 25 µM CldU (Sigma-Aldrich), 250 µM IdU (Sigma-Aldrich), 50 µM EdU (Invitrogen), 20 µM KU-55933 (Selleckchem), 10 mM HU (Sigma-Aldrich), 0,5 µM Camptothecin (Sigma-Aldrich), 25 µM Roscovitine (Sigma-Aldrich), 15 µM Cdc7 inhibitor (XL-413; Adooq Bioscience) and 1.5 mM thymidine (Sigma-Aldrich).

Gene silencing by siRNA

Transfections of the following siRNAs were performed with DharmaFECT™ (VWR) following manufacturer's guidelines: NON-TARGET (Dharmacon: D-001810-10-20) / FBH1 (Dharmacon: L-017404-00-0005) / SMARCAL1 #1 (Thermofisher: s26996) / SMARCAL1 #2 (Thermofisher: s26997) / ZRANB3 (Thermofisher: pool of s38486/s38487/s38488) / FANCM (Thermofisher: pool of s33619/s33620/s33621) / PRIMPOL #16 (Thermofisher: s47416) / PRIMPOL #17 (Thermofisher: s47417). All siRNA duplexes were used at 10nM final concentration unless specified otherwise.

Isolation of proteins on nascent DNA (iPOND)

An adapted version of iPOND that overcomes its efficiency limitation thanks to the use of superparamagnetic beads was performed as described previously [24]. Briefly, EdU-labelled and -treated cells were fixed in 1% PFA for 10 min and quenched with 0.125 mM glycine (pH 7) for 5 min at RT. Cells were harvested, pelleted by centrifugation and lysed in lysis buffer (ChIP Express kit, Active Motif) for 30 min at 4°C. Lysates were passed through a 21-gauge needle 10 times and the nuclei were pelleted by centrifugation, then rinsed with PBS supplemented with (Roche) before being subjected to click reaction for 30 min at RT with 0.2 mM biotin-azide (Invitrogen). After click reaction, nuclei were pelleted, rinsed with PBS + PIC, resuspended in shearing buffer (ChIP Express kit, Active Motif) and sonicated (Bioruptor, Diagenode) for 15 min at high intensity (30-s/30-s on/off pulses) to obtain 100 - 300bp size fragments. Streptavidin-conjugated Dynabeads M-280 (Invitrogen) were washed three times with 1x blocking buffer (1% Triton X-100, 2 mM EDTA (pH 8), 150 mM NaCl, 20 mM Tris-HCl (pH 8), 20 mM beta-glycerol phosphate, 2 mM sodium orthovanadate, PIC) and then blocked for 1 h at RT with blocking buffer containing 10 mg/mL salmon-sperm DNA (Sigma-Aldrich). Lysates were then incubated with previously blocked Dynabeads (1:10) for 30 min at RT. Finally, beads were washed twice with washing buffer (containing 150 mM NaCl) and twice with high-salt washing buffer (containing 500 mM NaCl) before the proteins were eluted in Laemmli buffer for analysis by either MS or immunoblot.

See also Supplementary Materials and Methods.

Immunoprecipitation and immunoblots

Chromatin fractions were obtained as described in [25] and incubated with 5 µg of anti-MCM3 antibody (homemade) or 5 µg of rabbit immunoglobulin Gs (IgG, Sigma, I8140) for 1 h at 4ºC in rotation. Protein immunocomplexes were pulled down with Pierce® Protein A Agarose beads (Thermo Scientific, 20333), washed with washing buffer (50 mM Tris pH 7.4, 1501 mM NaCl, 1 mM EDTA and 1% triton) and eluted in Laemmli buffer.

Total lysates were harvested in 2% SDS-containing 67 mM Tris-HCl (pH 6.8) buffer. Samples were boiled for 15 min, protein content was measured and then samples were normalized and diluted in Laemmli buffer.

Proteins were separated by SDS-PAGE and transferred to nitrocellulose membranes in accordance with standard protocols. Antibodies against the indicated proteins were diluted in blocking solution (0.05% Tween 20-containing TBS supplemented with 3% skimmed milk powder) as follows: MCM6 (sc-9843; 1/200), Cdc45 (sc-20685; 1/200), PCNA (ab18197; 1/1000), Fen1 (BD-611294; 1/1000), RFC3 (ab154899; 1/1000),

RPA32 (#2208; 1/1000), Pan-MCM (A303-477A; 1/1000), MCM2 (sc-10771; 1/200), Pol δ (ab10362; 1/1000), Pol α (sc-5921; 1/200), Psf3 (A304-124A; 1/1000) GAP120 (sc-63; 1/100), P-Chk2 T68 (NB100-92502; 1/1000), p53 (MS-186; 1/1000), CtIP (A300488a; 1/1000), Rad51 (sc-8349; 1/200), BRCA2 (ab123491; 1/2000), FANCD2 (ab2187; 1/5000), SMC1 (A300-055A; 1/1000), SMC3 (A300-060A; 1/1000), SMARCAL1 (sc-376377; 1/500), Lamin B (sc-6217; 1/200), Actin (sc-8432; 1/2000) and H3 (ab1791; 1/2000).
For FBH1 detection, membranes were blocked in PBS-Tween (0.01% Tween-20 containing PBS) supplemented with 3% bovine serum albumin and incubated with FBH1 (sc-81563; 1/100) or Vinculin (sc-25336; 1/500) antibodies diluted in PBS-Tween, supplemented with 5% skimmed milk powder.

Flow cytometry
Cells were synchronized, labelled and treated as indicated in the corresponding figure legend. After that, cells were collected by trypsinization and fixed in 70% ethanol for at least 2 h at -20ºC before staining them with BrdU antibody (anti- BrdU, Abcam, ab6326; 1/ 250). DNA was counterstained with RNAse-containing 1% PI (Sigma-Aldrich).

Chromatin-enriched fraction isolation
Chromatin-enriched fractions were obtained as described in [23], and then chromatin-enriched fractions were processed and analyzed by immunoblot, as before.

DNA fiber assay
DNA fiber assay was performed in accordance with a protocol described in [2]. Abcam (ab6326; 1/1000) and Becton Dickinson (347580; 1/200) anti-BrdU antibodies were used for CldU and IdU labelling, respectively. Images were obtained using Leica TCS-SL confocal microscopy with a 63× oil immersion objective, and then analyzed using Fiji software. The number of fibers analyzed in each experiment is indicated in the corresponding figure legend.

QIBC
QIBC experiments were performed as described in [7]. Briefly, cells were pre-extracted with 0.5% Triton X-100-PBS for 1 min at 4ºC and fixed in 4% PFA for 10 min at RT. Cells were then incubated with anti-BrdU (Becton Dickinson; 1/50), anti-RPA (Homemade; 1/1000) and anti-YH2AX (Millipore; 1/2000) primary antibodies for 1 h at RT and with Alexa Fluor Plus secondary antibodies for a further 1 h at RT. Images were obtained with a motorized Olympus IX-81 wide-field microscope. Automated unbiased image acquisition was carried out with the proprietary Scan Acquisition software.

BrdU immunofluorescence under native conditions
BrdU-labelled and -treated cells were rinsed with PBS, pre-extracted with 0.5% Triton X-100-PBS for 10 min at 4ºC, and then fixed with 3% PFA / 2 %sucrose-PBS solution for 10 min at RT. After being washed with PBS, cells were blocked for 1 h at RT with 0.05% Tween 20-containing / 3% BSA-containing PBS. Cells were then incubated with the anti-BrdU (Becton Dickinson; 1/50) antibody diluted in blocking solution for 1 h at 37ºC, washed with blocking solution for 15 min at RT, and then incubated with the secondary antibody (anti-mouse 488; 1/500) for 20 min at 37ºC. Finally, cells were washed with blocking solution for 15 min at RT and DNA was counterstained with 0.1mg/mL RNAse-containing 1% (15 min at 37ºC). BrdU staining was analyzed by confocal microscopy and intensity measured using Image J software. Data from 4 different experiments were normalized based on the control conditions and statistical analysis (t-students) performed with all data grouped.

Pulsed-field gel electrophoresis (PFGE)
Cells were washed with PBS, trypsinized and resuspended at 8.33 × 106 cells/ml cell density in incubation buffer (0.25 mM EDTA, 20 mM NaCl, 10 mM Tris, pH 7.5). This suspension (120 l) was mixed 1:1 with 1% low-melting point agarose (Sigma) to obtain two agarose inserts, each containing 0.5 × 106 cells. Cells in plugs were then lysed (0.25 mM EDTA, 20 mM NaCl, 10 mM Tris, pH 7.5, 1% N-laurylsarcosyl, 1 mg/ml proteinase K) for 48 h at 50°C, washed three times with TE buffer (10 mM Tris, 1 mM EDTA, pH 7.5) and

run in 1% agarose gel (chromosomal grade; Bio-Rad) in a CHEF DR III PFGE apparatus (Bio-Rad; 120 angle; 60–240 s switch time; 4 V/cm) at 14◦C for 20 h. Finally, gels were stained with SYBRR Safe (Invitrogen) and analyzed with the LAS-4000 system (Fujifilm).

Agarose gels

DNA was run at 100V in 1.5% agarose gels to analyze sample sonication. DNA was stained with SYBRTM Safe (Invitrogen) and analyzed with Gel Doc™ EZ Imager (BioRad).

Statistical analysis

All statistical analyses were performed using GraphPad Prism 6 software. Paired or unpaired t-test analyses were performed as indicated. Values marked with asterisks are significantly different: *$p < 0.05$, **$p < 0.01$, ***$p < 0.001$, ****$p < 0.0001$). n.s. was used to indicate an absence of statistical significance.

Results

Analysis of nascent DNA-bound proteins after acute or sustained replication stress in non-transformed human cells

Isolation of proteins on nascent DNA (iPOND) [26] combined with mass spectrometry (MS) [14, 27] has been described as a powerful tool to characterize the human replisome and fork-associated proteins. Additionally, the development of more efficient versions of iPOND [24] has helped to address its limitation with respect to the need for liberal amounts of starting material and has extended its use to a wide range of cell lines. Thus, to define the changes at replication fork level that compromise fork stability in hTERT-RPE cells, we performed an iPOND-MS experiment that compared acute (2 h) and sustained (14 h) HU treatment (See Materials and Methods and Supplementary Materials and Methods for details). Importantly, we set up the experimental conditions to ensure that the DNA synthesis was completely inhibited. The following data confirms that DNA synthesis was completely inhibited after 15 min of 10 mM HU treatment: 1) no CldU/IdU incorporation is observed by DNA fiber analysis after this time [23]; 2) no progression through cell cycle is observed by flow cytometry analysis under these conditions (Fig. S1a); 3) no H3 immunoprecipitation is observed by iPOND when EdU is added after 15 min of HU treatment, which indicates that EdU is not incorporated into the DNA (Fig. S1b).

Remarkably, since HU takes 15 min to completely stall the replication forks of hTERT-RPE cells (Fig. S1b; lanes D and F), EdU was maintained in the media for the first 15 min of HU treatment (Fig. S1c). This prevents the labelled region from being displaced away from replication forks. The EdU incorporated during these first minutes of HU treatment increases the amount of labelled DNA (Fig. S1b; lanes B and D). Therefore, it was necessary to include a condition in which cells were harvested just after the initial 15 min of EdU+HU treatment (15' EdU/HU; Fig. S1c). The amount of incorporated EdU will be the same as in 2 h HU and 14 h HU in this case and thus, this condition is essential in order to properly analyze the HU-treated samples. The analysis was performed in triplicate in S-phase synchronized cells (to overcome the restriction in the amount of limited starting material) and $3x10^7$ hTERT-RPE cells were used in each condition.

A total of 716 proteins were identified by MS (Table S1). The pulse/chase enrichment ratios showed that the proteins most enriched at nascent DNA in the pulse condition included DNA polymerase δ, DNA polymerase ε, DNA primase, DNA ligase, RFC1, RFC2 and other replisome components, thereby validating the effectiveness of the proteomic approach taken for replisome component identification (Fig. S1d). To monitor the HU-induced changes, proteomic data were processed (Supplementary Materials and Methods) to generate a heatmap of protein abundance across the experimental conditions and, in addition, proteins were clustered according to their best-known function (Table S2). The 57% of the proteins considered nascent DNA-bound proteins in the pulse (because they present fold enrichments higher than two compared to the chase) had previously identified replication-related functions (Fig. S1e). Furthermore, the 81% of the proteins considered nascent DNA-bound proteins in the pulse in our proteomic analysis were also classified as nascent DNA-bound proteins in similar studies (Table S3), thus validating the reliability of our approach.

Replisome components are disengaged from nascent DNA upon acute HU treatment in hTERT-RPE cells

As expected, the results of the iPOND-MS experiment showed that most of the replisome components were enriched at nascent DNA in the pulse and 15'EdU/HU conditions (Fig. 1a), indicating that they were directly or indirectly associated to nascent DNA. Strikingly, most of them decreased their association with nascent DNA straight after an acute (2 h) HU treatment that does not compromise competence to restart [23].

Proteomic data was in most cases recapitulated by iPOND combined with western blot (WB) experiments (Fig. 1b). Consistent with the MS results, iPOND-WB experiments showed that MCM6 helicase was displaced away from nascent DNA after acute replication stress. Moreover, the iPOND-WB experiments confirmed that Cdc45, another component of the CMG complex that was not identified in our iPOND-MS experiment, was also displaced away from nascent DNA under this condition (Fig. 1b). According to our iPOND-MS experiments, not only the CMG, but also other replisome components such as those involved in lagging strand metabolism (DNA Ligase 1, DNA polymerase α, DNA polymerase δ, Fen1, Primase 2) were disengaged from nascent DNA upon 2 h HU treatment (Fig. 1a). Consistently, iPOND-WB experiment

showed that the association of Fen1 with nascent DNA was decreased upon HU treatment (Fig. 1b). Notably, in line with our previous data [23], proteins involved in maintaining fork stability and promoting their restart, such as Rad51, FANCD2 and SMC1/3 cohesins [2, 15–17, 19] were present in nascent DNA after acute but not sustained HU treatment (Fig. 1).

Replisome disengagement from nascent DNA results from HU-induced accumulation of parental ssDNA

The fact that the replisome components were displaced away from nascent DNA prompted us to analyze the way in which forks were remodeled after HU-induced acute replication stress. In human cells, HU-induced replication stress is believed to cause two different types of fork-remodeling events, functional uncoupling of helicases-polymerases and fork reversal, neither of which compromises fork restart [22]. Fork uncoupling would cause the accumulation of large amounts of ssDNA in the parental strand (Fig. S2a); by contrast, fork reversal would generate ssDNA in the nascent DNA strand (Fig. S2a).

To determine which of those remodeling events predominantly occurred upon acute HU treatment in hTERT-RPE cells, we analyzed the accumulation of ssDNA on each DNA strand. The analysis of ssDNA accumulation by native BrdU staining [28] showed a slight increase in nascent ssDNA upon acute HU treatment (Fig. 2a). In line with previous reports [22], this suggests that HU-induced replication stress leads to fork reversal in hTERT-RPE cells. Nonetheless, quantitative image-based cytometry (QIBC) [7] showed a much higher ssDNA accumulation in the parental strand than in the nascent strand under the same conditions (Fig. 2b and 2c). Moreover, an acute HU treatment was sufficient to induce the accumulation of large amounts of RPA on chromatin (Fig. S2b), which showed a good correlation with the amount of ssDNA detected by native BrdU staining in the parental but not in the nascent strand (Fig. S2c). Notably, in contrast to parental ssDNA, the amount of nascent ssDNA increased along with the HU treatment and reached its maximum once replication forks showed a clear accumulation of DNA breaks (Fig. 2c and S2d). These results strongly suggest that upon HU treatment, fork reversal is a rare event compare to fork uncoupling in hTERT-RPE cells. However, we cannot discard that the amount of ssDNA generated by each event is different. Hence, to confirm that fork uncoupling is the predominant event upon HU treatment, we analyzed the changes in the amount of parental and nascent ssDNA upon depletion of SMARCAL1[29, 30], FANCM[31], ZRANB3[32] or FBH1[33], translocases involved in fork reversal (Fig. 2d and S2e). As suggested by our previous results, this experiment discarded fork reversal as the predominant event upon HU treatment, since the depletion of the different translocases had none or very mild effect on decreasing the amount of nascent and on increasing the amount of parental ssDNA.

Besides fork uncoupling, ssDNA accumulation could also be explained by CtIP-induced fork resection [34]. However, we did not observe CtIP phosphorylation or RPA hyperphosphorylation upon acute HU treatment (Fig. S2F). Likewise nascent DNA degradation by Mre11 could also result in the accumulation of ssDNA in the parental strand [35]. Nonetheless, fiber analysis of cells treated with mirin (Mre11 inhibitor) [36] demonstrated that nascent DNA was not, at least largely, degraded upon acute HU treatment (Fig. S2G). Taken together, the above results suggest that helicase-polymerase uncoupling is the predominant remodeling event upon acute HU treatment.

hTERT-RPE cells maintain the competence to restart upon acute replication stress in the absence of CDK activity

As replisome components were absent in nascent DNA after acute replication stress (Fig. 1), we wondered whether the previously observed restart [23] was due to the activation of nearby origins, which cannot be distinguished in the fiber analysis due to their proximity to stalled forks [37]. To rule out this possibility, we performed DNA fiber analyses in which we inhibited activation of new origins by adding the CDK inhibitor Roscovitine [38] during the treatment and second labelling period [39–41]. The efficacy of Roscovitine was validated by the reduction in the number of new origin firing events (Fig. 3a). Moreover, consistent with a possible role of CDKs in the promotion of normal replication fork progression [42], the length of the IdU (second labelling) tracks was shorter in Roscovitine-treated samples (Fig. S3). Remarkably, the addition of Roscovitine did not impair competence to restart after acute replication stress (Fig. 3a), thus indicating that restart was not due to newly fired origins. To further confirm these results, we repeated the experiment with

Cdc7 inhibitor either alone or in combination with Roscovitine (Fig. 3b). As in the case of Roscovitine, the effect of the Cdc7 inhibitor was validated by the observed decrease in the number of new origin firing events. Notably, consistent with our previous results, none of the drugs impaired the ability to restart after a 2 h HU treatment.

PrimPol is a primase/polymerase that is able to re-prime DNA synthesis without the need of a 3'end, and consequently can synthesise the leading strand until it reaches the CMG complex [43–45]. To test whether this protein was contributing to the restart after a 2 h HU treatment, we tested the effect of its depletion by DNA fiber (Fig. S3b and S3c). In contrast to what occurs upon other genotoxic stresses, PrimPol does not seem to mediate the restart after a 2 h HU treatment.

CMG helicase maintains its integrity and association with chromatin after acute HU treatment

The fact that replication forks maintain their competence to restart in the absence of CDK activity (Fig. 3) when CMG is not associated with nascent DNA (Fig. 1 and S4) suggests that CMG helicase must be displaced away from nascent DNA but still present in chromatin, as the assembly of new CMG complexes is impaired under these conditions [42, 46]. Consistent with this, the analysis of chromatin-enriched fractions showed that CMG helicase remains associated with chromatin after acute HU treatment (Figure 4a). As expected, Roscovitine treatment decreased the association of Cdc45 and GINS with chromatin in untreated cells due to termination events (Fig. 4b). By contrast, CDK inhibition did not reduce their association with chromatin in HU-treated samples (Fig. 4b), which strongly supports the idea that the previously formed CMG helicase complexes remain associated with chromatin under these conditions. Consistent with the ability to restart in the presence of Roscovitine, and the fact that CMG helicase remains bound to chromatin under these conditions, co-IP experiments demonstrated that the integrity of the CMG complex is preserved upon acute HU treatment (Fig. 4c).

Analysis of the chromatin-bound fractions showed that other replisome components, such as those involved in lagging strand metabolism (DNA polymerase α, DNA polymerase δ and Fen1), also remained associated with chromatin upon acute HU treatment (Fig. 4a). Consistent with the accumulation of ssDNA observed in Fig. 2, chromatin-bound RPA levels increased upon 2 h HU treatment. In contrast, but in agreement with previous reports [14], association of PCNA with chromatin decreased straight after a 2 h HU treatment. Notably, most of the replisome components, including the CMG complex, decreased their association with chromatin upon a sustained HU treatment that compromises the ability to restart [23] (Fig. 4a). In line with this, Tipin and Claspin, which are involved in fork stability maintenance as part of the Replication Pausing Complex (RPC) [47], maintained their association with chromatin after a 2 h but not that much after a 14 h HU treatment. Likewise, Rad51, FANCD2 and SMC1/3 cohesins also decreased their association with chromatin only after a sustained replication stress (Fig. S4c).

Collectively, our results indicate that acute HU treatment does not challenge CMG integrity or its association to chromatin in hTERT-RPE cells, and suggest that fork restart is mediated by recycling previously formed CMG complexes.

Replication resumption after acute HU treatment does not result in the accumulation of under-replicated regions in hTERT-RPE cells

The above results indicate that, in line with previous reports [22], forks can be remodeled without compromising their ability to restart. Moreover, our data suggest that forks resume replication after acute HU-treatment using the same CMG complexes that had been disengaged from nascent DNA. To define the dynamics of replication resumption under these conditions, we analyzed ssDNA disappearance upon release from HU treatment by QIBC (Fig. 5a). The amount of parental ssDNA decreased almost completely after a 30 min release from HU treatment. Consistent with this, chromatin-bound RPA levels were similar to the control after a 30 min to 1 h release from acute HU treatment (Fig. S5a).

DNA replication under stress conditions can result in the accumulation of under-replicated regions, which leads to the presence of 53BP1 bodies in the subsequent G1 phase [48–50]. Thus, we wondered whether replication resumption after replisome disengagement from nascent DNA upon acute replication stress can also lead to the accumulation of under-replicated regions. Remarkably, the percentage of G1 cells presenting 53BP1 bodies did not significantly increased upon release from acute HU treatment (Fig. 5b). Notably,

consistent with the previously observed competence to restart after acute HU treatment, this was not due to changes in the number of cells arriving at G1 (Fig. S5b). Together, these results support the idea that replisome disengagement from nascent DNA upon acute HU treatment does not challenge replication or compromise genome integrity.

Discussion

The maintenance of genome integrity is essential for the existence of all organisms, and DNA replication is one of the events in which the genome is most vulnerable. Replication forks stall frequently as a result of encounters between the replication machinery and different obstacles in the DNA template or a lack of basic elements to replicate the DNA, such as nucleotides. While preventing the restart of stalled forks may negatively influence the proliferative capacity of cells and runs the risk of genomic information being lost, their restart may also lead to the acquisition of mutations, since some restart pathways are error prone [51–53]. In this regard, the mechanisms involved in maintaining the ability to restart and their regulation remain unclear. Likewise, the fate of the replisome machinery during replication stress is still controversial [10–13]. To clarify previous concerns, we decided to perform a comparative iPOND-MS analysis of the proteins associated with replication forks under these conditions, while taking into account our previous data showing that the ability to restart is compromised in non-transformed human cells after sustained but not acute replication stress [23].

Interestingly, using an improved version of iPOND [24] we show here that replisome components of non-transformed human hTERT-RPE cells, including the CMG helicase, are disengaged from nascent DNA but still present in chromatin after acute replication stress (Figure 5c). Notably, fork stability-related proteins such as Rad51, FANCD2 and SMC1/3 [2, 15–17, 19] increase their association with nascent DNA under these conditions, thus indicating that replisome components are being specifically displaced. These results, together with the fact that cells maintain the competence to restart under these conditions, indicate that replisome disengagement from nascent DNA does not result in fork collapse. It has previously been reported by Dungrawala and colleagues [14] that most of the replisome components are stably bound to nascent DNA, and only decrease due to termination events upon 3mM HU treatment in HEK293T cells. This discrepancy could be related to the different experimental setting or the use of a different cellular model. On the one hand, they use a dose of HU that does not fully block EdU incorporation and thus, EdU is maintained in the media during the treatment thereby making it possible to label newly fired forks. By contrast, in our experiment, we use a dose of HU that completely blocks EdU incorporation after 15 min of treatment (Ercilla et al., 2016) (Fig. S1b). On the other hand, our analysis was performed in non-transformed human cells, while theirs was carried out in HEK293T tumor cells. As already noted by Dungrawala and colleagues [14], the replication rate in untreated conditions is 3-fold slower in HEK293T than in hTERT-RPE cells, which would affect the speed of unwinding and therefore, the helicase-polymerase uncoupling. Thus, we cannot exclude that the observed discrepancy might also be due to differences between cell types.

Remarkably, the association of the replisome components with chromatin is in most cases only lost after a sustained replication stress that compromises the ability to restart. The fact that replisome components are bound to chromatin after acute HU treatment in the presence of Roscovitine, which prevents the activation of new origins [39–41], rules out the possibility of new origin firing masking their loss. Our data also show that the integrity of the CMG complex is maintained upon acute HU treatment; this, together with the fact that replication forks are able to restart under these conditions even in the presence of Roscovitine and/or Cdc7 inihibitor, in which the formation of new complexes must be abrogated [42, 46], supports the idea that CMG helicase remains associated with chromatin in order to be recycled during restart.

The fact that replisome components are disengaged from nascent DNA but still present in chromatin upon acute replication stress implies that replication forks might have been remodeled. It has previously been reported that HU can cause two different types of fork remodeling events that do not compromise fork restart: fork reversal and fork uncoupling [22]. In this regard, our results show that there is ssDNA exposed in the nascent strand upon 2 h HU treatment [33], which strongly suggests the presence of reversed forks upon acute replication stress in hTERT-RPE cells. However, the increase in chromatin-bound RPA levels upon acute replication stress cannot be explained by reversed forks. Additionally, depletion of translocases known to be involved in fork reversal had only a mild effect in the amount of parental and nascent ssDNA exposed upon 2 h HU treatment. Moreover, the presence of high amounts of ssDNA in the parental DNA strand rather suggests that most of the forks are uncoupled. Consistent with this, there is a strong correlation between chromatin-bound RPA levels and the ssDNA in the parental strand. Accumulation of parental ssDNA could also be due to resection. Nonetheless, the amount of ssDNA present in the parental strand is not time-

dependent and no clear increase in resection marks such as P-CtIP and P-RPA is observed. Likewise, Mre11-dependent DNA degradation may also cause ssDNA accumulation in the parental strand [35] but, in contrast to sustained HU treatment, we show that acute treatment does not cause Mre11-dependent DNA degradation in hTERT-RPE cells. Taken together, these data suggest that fork uncoupling is the predominant remodeling event upon HU-induced acute replication stress in hTERT-RPE cells.

Functional helicase-polymerase uncoupling is believed to occur in response to a variety of genotoxic stresses in several species, including humans [22, 54]. In fact, the ssDNA that accumulates during this process is thought to be required to induce the activation of the checkpoint response [55]. In this regard, it has generally been considered that uncoupling might cause an extended loop of ssDNA without compromising the interaction between nascent DNA and the replisome. However, our data show that replisome components are disengaged from nascent DNA during this process (Figure 5c). Notably, this disengagement does not compromise fork restart, thereby suggesting that replication forks are much more dynamic than initially expected. Interestingly, a recent study using an in vitro prokaryotic DNA replication system [56] shows that leading- and lagging-strand machineries work uncoupled from each other. Their data show that, at least in prokaryotes, leading- and lagging-strand DNA polymerases function independently within a single replisome. Notably, the stochastic function of each polymerase results in its transient disengagement from the replicative helicase without blocking replication fork progression, thus demonstrating the high plasticity of replication forks.

Our data clearly show that, after acute replication stress, eukaryotic replication forks can be restarted despite the disengagement of replisome components from nascent DNA. The lagging strand per se has a discontinuous back-stitching DNA synthesis mechanism and could therefore easily be reinitiated by DNA polymerase α. By contrast, leading-strand DNA synthesis occurs in a continuous manner, thereby challenging its restart. In this regard, one possibility to restart leading-strand synthesis would be to reinitiated DNA synthesis from the site where the replisome is situated. This would generate long gaps of under-replicated ssDNA behind the fork that could be repaired by Rad51-mediated mechanisms in G2 [57, 58]. In agreement with this, it has been reported that HU causes the accumulation of post-replicative ssDNA gaps in hTERT-RPE cells that could be reflecting DNA synthesis restart at a different distance from the original block [22]; however, we have also shown that the bulk of ssDNA disappears rapidly once replication is reinitiated. Another possibility to resume leading-strand DNA synthesis would be to re-engage DNA polymerase ε with the 3' end of the nascent strand. DNA polymerase ε is strongly associated with CMG [59] and thus, in order to engage it with the nascent 3' terminus, a linker molecule might be needed to bring the replisome close to the DNA end. Alternatively, the soluble store of DNA polymerase δ could also be engaged to the 3' end of the nascent strand and carry on the DNA synthesis until it reaches the slow-moving CMG complex, when it would be dissociated by collision release and DNA synthesis would be continued by the DNA polymerase ε [60]. Finally, similarly to what occurs upon UV light-induced damage, re-priming of PrimPol or DNA polymerase α could also promote DNA synthesis until the end terminus of the nascent DNA is engaged with the replisome. In this case, the re-priming events could generate small gaps behind the fork that would be filled by other polymerases or repaired by HR [43–45, 61]. Nonetheless, our results indicate that at least PrimPol does not seem to be involved in the restart after a 2 h HU treatment.

Regardless of the mechanism, it is relevant that reinitiation occurs after the disengagement of replisome components from nascent DNA, and that this does not seem to compromise genomic instability, since an increase in 53BP1 foci-containing cells in G1 is not observed. As previously mentioned, during the last years, increasing evidences support the idea of replication forks being much more plastic than what one could initially expect. Recent studies have shown for instance that replication forks can reverse without compromising their ability to restart [22] or that, at least in vitro, leading- and lagging-strand DNA polymerases function independently within a single replisome [56]. In line with this, we show here that, replication forks of non-transformed hTERT-RPE cells are more plastic and resilient than expected, and that they can restart from a situation involving disengagement of replisome components from nascent DNA, apparently without inducing genomic instability.

Acknowledgement

We thank Dr. Surrallés for Fen1, Dr. Mendéz for MCM3 and Dr. Stracker for SMC1 and Pan-MCM antibodies. We also thank the members of our laboratory for their discussion and the advanced optical microscopy unit of the CCiT-UB for its technical assistance.

This work was supported by the grants from the Ministerio de Economia y Competitividad (SAF2013-42742-R, SAF2016-76239-R) for N.A; a FPI fellowship from the Ministerio de Ciencia e Innovación for A.E. and A.Ll.; and a FI fellowship from the Generalitat de Catalunya for S.F.

Competing interests

The authors declare no competing interests.

References

1. Branzei D, Foiani M (2009) The checkpoint response to replication stress. DNA Repair (Amst) 8:1038–1046. https://doi.org/10.1016/j.dnarep.2009.04.014
2. Petermann E, Orta MLL, Issaeva N, et al (2010) Hydroxyurea-stalled replication forks become progressively inactivated and require two different RAD51-mediated pathways for restart and repair. Mol Cell 37:492–502. https://doi.org/10.1016/j.molcel.2010.01.021
3. Cortez D (2015) Preventing Replication Fork Collapse to Maintain Genome Integrity. DNA Repair (Amst) 32:149–57. https://doi.org/10.1016/j.dnarep.2015.04.026
4. Sakofsky CJ, Ayyar S, Malkova A (2012) Break-induced replication and genome stability. Biomolecules 2:483–504. https://doi.org/10.3390/biom2040483
5. Zou L, Elledge SJ (2003) Sensing DNA damage through ATRIP recognition of RPA-ssDNA complexes. Science 300:1542–8. https://doi.org/10.1126/science.1083430
6. Liu Q, Guntuku S, Cui X-S, et al (2000) Chk1 is an essential kinase that is regulated by Atr and required for the G2/M DNA damage checkpoint. Genes & Dev 14:1448–1459. https://doi.org/10.1101/gad.14.12.1448
7. Toledo LI, Altmeyer M, Rask M-B, et al (2013) ATR prohibits replication catastrophe by preventing global exhaustion of RPA. Cell 155:1088–103. https://doi.org/10.1016/j.cell.2013.10.043
8. Lossaint G, Larroque M, Ribeyre C, et al (2013) FANCD2 Binds MCM Proteins and Controls Replisome Function upon Activation of S Phase Checkpoint Signaling. Mol Cell 51:678–690. https://doi.org/10.1016/j.molcel.2013.07.023
9. Forment J V, Blasius M, Guerini I, Jackson SP (2011) Structure-specific DNA endonuclease Mus81/Eme1 generates DNA damage caused by Chk1 inactivation. PLoS One 6:e23517. https://doi.org/10.1371/journal.pone.0023517
10. Cobb JA, Bjergbaek L, Shimada K, et al (2003) DNA polymerase stabilization at stalled replication forks requires Mec1 and the RecQ helicase Sgs1. EMBO J 22:4325–36. https://doi.org/10.1093/emboj/cdg391
11. Cobb JA, Schleker T, Rojas V, et al (2005) Replisome instability, fork collapse, and gross chromosomal rearrangements arise synergistically from Mec1 kinase and RecQ helicase mutations. Genes Dev 19:3055–69. https://doi.org/10.1101/gad.361805
12. Lucca C, Vanoli F, Cotta-Ramusino C, et al (2004) Checkpoint-mediated control of replisome-fork association and signalling in response to replication pausing. Oncogene 23:1206–13. https://doi.org/10.1038/sj.onc.1207199
13. De Piccoli G, Katou Y, Itoh T, et al (2012) Replisome stability at defective DNA replication forks is independent of S phase checkpoint kinases. Mol Cell 45:696–704. https://doi.org/10.1016/j.molcel.2012.01.007
14. Dungrawala H, Rose KL, Bhat KP, et al (2015) The Replication Checkpoint Prevents Two Types of Fork Collapse without Regulating Replisome Stability. Mol Cell 59:998–1010. https://doi.org/10.1016/j.molcel.2015.07.030
15. Remeseiro S, Losada A (2013) Cohesin, a chromatin engagement ring. Curr Opin Cell Biol 25:63–71. https://doi.org/10.1016/j.ceb.2012.10.013
16. Wu N, Yu H (2012) The Smc complexes in DNA damage response. Cell Biosci 2:5. https://doi.org/10.1186/2045-3701-2-5
17. Hashimoto Y, Ray Chaudhuri A, Lopes M, Costanzo V (2010) Rad51 protects nascent DNA from Mre11-dependent degradation and promotes continuous DNA synthesis. Nat Struct Mol Biol 17:1305–11. https://doi.org/10.1038/nsmb.1927
18. Schlacher K, Christ N, Siaud N, et al (2011) Double-strand break repair-independent role for BRCA2 in blocking stalled replication fork degradation by MRE11. Cell 145:529–42. https://doi.org/10.1016/j.cell.2011.03.041
19. Schlacher K, Wu H, Jasin M (2012) A Distinct Replication Fork Protection Pathway Connects Fanconi Anemia Tumor Suppressors to RAD51-BRCA1/2. Cancer Cell 22:106–116. https://doi.org/10.1016/j.ccr.2012.05.015
20. Quinet A, Lemaçon D, Vindigni A (2017) Replication Fork Reversal: Players and Guardians. Mol Cell 68:830–833. https://doi.org/10.1016/j.molcel.2017.11.022
21. Thangavel S, Berti M, Levikova M, et al (2015) DNA2 drives processing and restart of reversed replication forks in human cells. J Cell Biol 208:545–62. https://doi.org/10.1083/jcb.201406100
22. Zellweger R, Dalcher D, Mutreja K, et al (2015) Rad51-mediated replication fork reversal is a global response to genotoxic treatments in human cells. J Cell Biol 208:563–79. https://doi.org/10.1083/jcb.201406099

23. Ercilla A, Llopis A, Feu S, et al (2016) New origin firing is inhibited by APC/CCdh1 activation in S-phase after severe replication stress. Nucleic Acids Res. https://doi.org/10.1093/nar/gkw132
24. Aranda S, Rutishauser D, Ernfors P (2014) Identification of a large protein network involved in epigenetic transmission in replicating DNA of embryonic stem cells. Nucleic Acids Res 42:6972–86. https://doi.org/10.1093/nar/gku374
25. Méndez J, Stillman B (2000) Chromatin association of human origin recognition complex, cdc6, and minichromosome maintenance proteins during the cell cycle: assembly of prereplication complexes in late mitosis. Mol Cell Biol 20:8602–12. https://doi.org/10.1128/MCB.20.22.8602-8612.2000
26. Sirbu BM, Couch FB, Feigerle JT, et al (2011) Analysis of protein dynamics at active, stalled, and collapsed replication forks. Genes Dev 25:1320–7. https://doi.org/10.1101/gad.2053211
27. Lopez-Contreras AJ, Ruppen I, Nieto-Soler M, et al (2013) A proteomic characterization of factors enriched at nascent DNA molecules. Cell Rep 3:1105–16. https://doi.org/10.1016/j.celrep.2013.03.009
28. Couch FB, Bansbach CE, Driscoll R, et al (2013) ATR phosphorylates SMARCAL1 to prevent replication fork collapse. Genes Dev 27:1610–23. https://doi.org/10.1101/gad.214080.113
29. Kolinjivadi AM, Sannino V, De Antoni A, et al (2017) Smarcal1-Mediated Fork Reversal Triggers Mre11-Dependent Degradation of Nascent DNA in the Absence of Brca2 and Stable Rad51 Nucleofilaments. Mol Cell 867–881. https://doi.org/10.1016/j.molcel.2017.07.001
30. Taglialatela A, Alvarez S, Leuzzi G, et al (2017) Restoration of Replication Fork Stability in BRCA1- and BRCA2-Deficient Cells by Inactivation of SNF2-Family Fork Remodelers. Mol Cell 68:414-430.e8. https://doi.org/10.1016/j.molcel.2017.09.036
31. Gari K, Decaillet C, Delannoy M, et al (2008) Remodeling of DNA replication structures by the branch point translocase FANCM. Proc Natl Acad Sci 105:16107–16112. https://doi.org/10.1073/pnas.0804777105
32. Vujanovic M, Krietsch J, Raso MC, et al (2017) Replication Fork Slowing and Reversal upon DNA Damage Require PCNA Polyubiquitination and ZRANB3 DNA Translocase Activity. Mol Cell 67:882-890.e5. https://doi.org/10.1016/j.molcel.2017.08.010
33. Fugger K, Mistrik M, Neelsen KJ, et al (2015) FBH1 Catalyzes Regression of Stalled Replication Forks. Cell Rep 10:1749–1757. https://doi.org/10.1016/j.celrep.2015.02.028
34. Sartori AA, Lukas C, Coates J, et al (2007) Human CtIP promotes DNA end resection. Nature 450:509–14. https://doi.org/10.1038/nature06337
35. Hashimoto Y, Puddu F, Costanzo V (2012) RAD51- and MRE11-dependent reassembly of uncoupled CMG helicase complex at collapsed replication forks. Nat Struct Mol Biol 19:17–24. https://doi.org/10.1038/nsmb.2177
36. Lemaçon D, Jackson J, Quinet A, et al (2017) MRE11 and EXO1 nucleases degrade reversed forks and elicit MUS81-dependent fork rescue in BRCA2-deficient cells. Nat Commun 8:. https://doi.org/10.1038/s41467-017-01180-5
37. Fragkos M, Ganier O, Coulombe P, Méchali M (2015) DNA replication origin activation in space and time. Nat Rev Mol Cell Biol 16:360–74. https://doi.org/10.1038/nrm4002
38. Meijer L, Borgne A, Mulner O, et al (1997) Biochemical and cellular effects of roscovitine, a potent and selective inhibitor of the cyclin-dependent kinases cdc2, cdk2 and cdk5. Eur J Biochem 243:527–536. https://doi.org/10.1111/j.1432-1033.1997.t01-2-00527.x
39. Ilves I, Petojevic T, Pesavento JJ, Botchan MR (2010) Activation of the MCM2-7 helicase by association with Cdc45 and GINS proteins. Mol Cell 37:247–58. https://doi.org/10.1016/j.molcel.2009.12.030
40. Kumagai A, Shevchenko A, Shevchenko A, Dunphy WG (2011) Direct regulation of Treslin by cyclin-dependent kinase is essential for the onset of DNA replication. J Cell Biol 193:995–1007. https://doi.org/10.1083/jcb.201102003
41. Kumagai A, Shevchenko A, Shevchenko A, Dunphy WG (2010) Treslin collaborates with TopBP1 in triggering the initiation of DNA replication. Cell 140:349–59. https://doi.org/10.1016/j.cell.2009.12.049
42. Labib K (2010) How do Cdc7 and cyclin-dependent kinases trigger the initiation of chromosome replication in eukaryotic cells? Genes Dev 24:1208–19. https://doi.org/10.1101/gad.1933010
43. Bianchi J, Rudd SG, Jozwiakowski SK, et al (2013) Primpol bypasses UV photoproducts during eukaryotic chromosomal DNA replication. Mol Cell 52:566–573. https://doi.org/10.1016/j.molcel.2013.10.035
44. Mourón S, Rodriguez-Acebes S, Martínez-Jiménez MI, et al (2013) Repriming of DNA synthesis at stalled replication forks by human PrimPol. Nat Struct Mol Biol 20:1383–9. https://doi.org/10.1038/nsmb.2719

45. García-Gómez S, Reyes A, Martínez-Jiménez MII, et al (2013) PrimPol, an Archaic Primase/Polymerase Operating in Human Cells. Mol Cell 52:541–553. https://doi.org/10.1016/j.molcel.2013.09.025
46. Araki H (2010) Cyclin-dependent kinase-dependent initiation of chromosomal DNA replication. Curr Opin Cell Biol 22:766–71. https://doi.org/10.1016/j.ceb.2010.07.015
47. Errico A, Costanzo V (2012) Mechanisms of replication fork protection: a safeguard for genome stability. Crit Rev Biochem Mol Biol 47:222–235. https://doi.org/10.3109/10409238.2012.655374
48. Lukas C, Savic V, Bekker-Jensen S, et al (2011) 53BP1 nuclear bodies form around DNA lesions generated by mitotic transmission of chromosomes under replication stress. Nat Cell Biol 13:243–253. https://doi.org/10.1038/ncb2201
49. Harrigan JA, Belotserkovskaya R, Coates J, et al (2011) Replication stress induces 53BP1-containing OPT domains in G1 cells. J Cell Biol 193:97–108. https://doi.org/10.1083/jcb.201011083
50. Moreno A, Carrington JT, Albergante L, et al (2016) Unreplicated DNA remaining from unperturbed S phases passes through mitosis for resolution in daughter cells. Proc Natl Acad Sci U S A 1603252113-. https://doi.org/10.1073/pnas.1603252113
51. Marians KJ (2018) Lesion Bypass and the Reactivation of Stalled Replication Forks. 1–22
52. Zeman MK, Cimprich KA (2014) Causes and consequences of replication stress. Nat Cell Biol 16:2–9. https://doi.org/10.1038/ncb2897
53. Macheret M, Halazonetis TD (2015) DNA replication stress as a hallmark of cancer. Annu Rev Pathol 10:425–48. https://doi.org/10.1146/annurev-pathol-012414-040424
54. Byun TS, Pacek M, Yee MC, et al (2005) Functional uncoupling of MCM helicase and DNA polymerase activities activates the ATR-dependent checkpoint. Genes Dev 19:1040–1052. https://doi.org/10.1101/gad.1301205
55. Cortez D (2005) Unwind and slow down: Checkpoint activation by helicase and polymerase uncoupling. Genes Dev 19:1007–1012. https://doi.org/10.1101/gad.1316905
56. Graham JE, Marians KJ, Kowalczykowski SC (2017) Independent and Stochastic Action of DNA Polymerases in the Replisome. Cell 169:1201-1213.e17. https://doi.org/10.1016/j.cell.2017.05.041
57. Su X, Bernal JA, Venkitaraman AR (2008) Cell-cycle coordination between DNA replication and recombination revealed by a vertebrate N-end rule degron-Rad51. Nat Struct Mol Biol 15:1049–1058. https://doi.org/10.1038/nsmb.1490
58. González-Prieto R, Muñoz-Cabello AM, Cabello-Lobato MJ, Prado F (2013) Rad51 replication fork recruitment is required for DNA damage tolerance. EMBO J 32:1307–1321. https://doi.org/10.1038/emboj.2013.73
59. Sun J, Shi Y, Georgescu RE, et al (2015) The architecture of a eukaryotic replisome. Nat Struct Mol Biol 22:976–982. https://doi.org/10.1038/nsmb.3113
60. Schauer GD, O'Donnell ME (2017) Quality control mechanisms exclude incorrect polymerases from the eukaryotic replication fork. Proc Natl Acad Sci 114:675–680. https://doi.org/10.1073/pnas.1619748114
61. Elvers I, Johansson F, Groth P, et al (2011) UV stalled replication forks restart by re-priming in human fibroblasts. Nucleic Acids Res 39:7049–57. https://doi.org/10.1093/nar/gkr420
62. Sirbu BM, McDonald WH, Dungrawala H, et al (2013) Identification of proteins at active, stalled, and collapsed replication forks using isolation of proteins on nascent DNA (iPOND) coupled with mass spectrometry. J Biol Chem 288:31458–67. https://doi.org/10.1074/jbc.M113.511337
63. Alabert C, Bukowski-Wills J-C, Lee S-B, et al (2014) Nascent chromatin capture proteomics determines chromatin dynamics during DNA replication and identifies unknown fork components. Nat Cell Biol 16:281–293. https://doi.org/10.1038/ncb2918
64. Wang G, Wu WW, Zeng W, et al (2006) Label-free protein quantification using LC-coupled ion trap or FT mass spectrometry: Reproducibility, linearity, and application with complex proteomes. J Proteome Res 5:1214–23. https://doi.org/10.1021/pr050406g
65. Mi H, Muruganujan A, Casagrande JT, Thomas PD (2013) Large-scale gene function analysis with the PANTHER classification system. Nat Protoc 8:1551–66. https://doi.org/10.1038/nprot.2013.092

Figure Legends

Fig. 1 Replisome is disengaged from nascent DNA upon acute HU treatment in hTERT-RPE cells. (a) The protein ID of the replisome components and the DNA repair-related proteins identified in the iPOND-MS experiment and their normalized relative abundance in each condition are represented. (b) Cells were treated and harvested as in (a). The proteins present in iPOND extracts were analyzed by WB with the indicated antibodies. Input: nuclear extract. Histone 3 (H3) was used as an immunoprecipitation control. l.e.: long exposure. s.e.: short exposure. (-): negative control (no EdU). Pulse: 15 min EdU; Chase: pulse followed by 2 h with low dose thymidine. For experimental setting detail see also Fig. S1 and Tables S1, S2 and S3

Fig. 2 Acute HU treatment generates large amounts of parental ssDNA. (a) S-phase synchronized cells were labelled for 10 min with BrdU and treated with HU during the indicated time before performing BrdU immunofluorescence under native conditions. DNA was counterstained with propidium iodide (PI). The relative BrdU intensities (in arbitrary units (a.u.)), of more than 600 cells were measured in each condition. Box and whiskers show: min, max, median and first quartiles. Representative images are shown (left panel). (b, c) Asynchronously growing cells were labelled for 48 h (parental ssDNA) or 15 min (nascent ssDNA) with BrdU and treated for the indicated time with HU or left untreated (control). For parental ssDNA detection, cells were released overnight in 10 uM thymidine before HU treatment. For nascent ssDNA detection, BrdU was maintained in the media for the first 15 min of HU treatment. BrdU under native conditions was analyzed with QIBC. Cells were counterstained with DAPI. The relative BrdU intensities (in arbitrary units (a.u.)), of at least 5000 cells were measured in each condition (unpaired t-test). (d) Cells were transfected with the indicated siRNAs for 48h and labelled and treated as in b and c. The average relative BrdU intensities (in arbitrary units (a.u.)) of more 5000 cells are shown. NT: Non-Target. See also Fig. S2

Fig. 3 hTERT-RPE cells maintain the competence to restart upon acute replication stress in the absence of CDK activity. (a, b) Asynchronously growing cells were labelled and treated as indicated. DNA fibers were prepared and stained. The percentage of stalled, restarted and new origin firing events is shown. Around 1500 fibers were counted in each condition. Error bars represent standard deviation (paired t-test, n=3). Representative images are shown (bottom-right panel). Cdc7i: Cdc7 inhibitor. See also Fig. S3

Fig. 4 CMG helicase maintains its integrity and association with chromatin after acute HU treatment (a, b) Cells were synchronized in S phase (Cs) and then treated with HU for the indicated time or left untreated. Chromatin-enriched fractions were analyzed by WB with the indicated antibodies. Roscovitine was added where indicated. Input: whole cell lysates. Lamin B and Histone 3 (H3) were used as loading control. Pol: polymerase. (c) S-phase synchronized cells were treated with HU for the indicated time or left untreated (Cs). Chromatin fractions were incubated with antibodies against MCM3 or non-specific IgG. Protein immunocomplexes were pulled down and analyzed by WB with the indicated antibodies. See also Fig. S4

Fig. 5 Replication resumption after an acute HU treatment does not result in the accumulation of under-replicated regions in hTERT-RPE cells. (a) Asynchronously growing cells were labelled for 48 h with BrdU and released overnight in 10 uM thymidine before HU treatment. After that, cells were treated for 2 h with HU and then released into fresh media for the indicated time. BrdU under native conditions was analyzed by QIBC. Cells were counterstained with DAPI. The relative BrdU intensities (in arbitrary units (a.u.) of at least 5000 cells were measured in each condition (unpaired t-test, relative to 2 h HU). (b) S-phase synchronized cells were treated for the indicated time with HU or left untreated (Cs), and then released (R) for 12 h into fresh medium. Representative images are shown (left panel). The arrows indicate double positive cells. The average percentage of 53BP1 foci (>6) and cyclin D1 (CycD1) double-positive cells relative to total G1 (cyclin D1-positive) cells is shown (right panel). Error bars represent standard deviation, (paired t-test, n=3). More than 1000 cells were analyzed in each condition. (c) The current model proposes 2 types of remodeling events upon 2 h HU treatment: functional helicase/polymerase uncoupling and fork reversal. Our data shows that an open replication fork, were replisome components are disengage from nascent DNA, is the predominant remodeling event upon 2 h HU treatment. In addition, our data also shows that replication forks

maintain the competence to restart after this remodeling. > stands for “more than”; < stands for “minus than”.
See also Fig. S5

Figure 1.

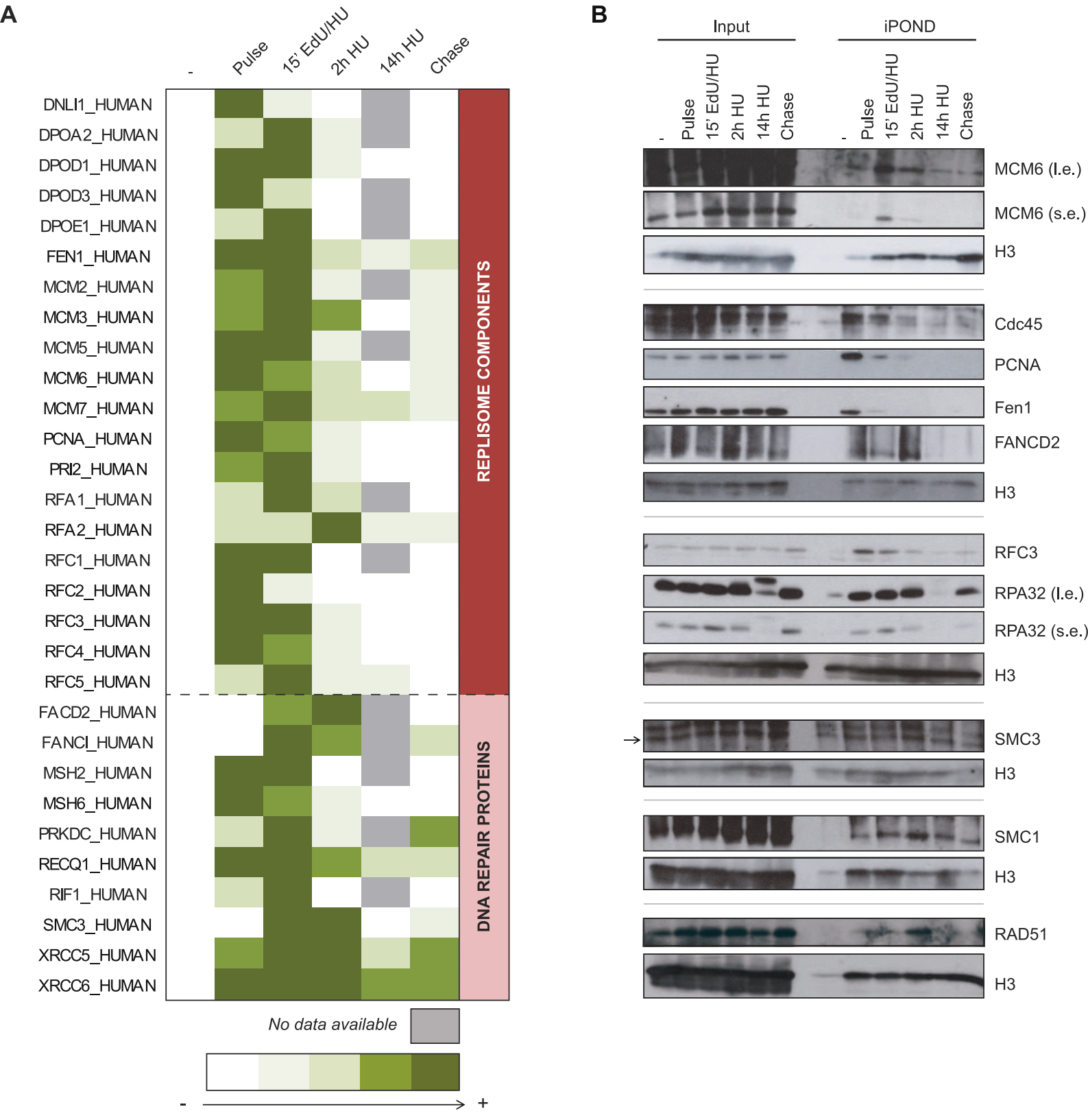
A
-
Pulse
15' EdU/HU
2h HU
14h HU
Chase
DNLI1_HUMAN
DPOA2_HUMAN
DPOD1_HUMAN
DPOD3_HUMAN
DPOE1_HUMAN
FEN1_HUMAN
MCM2_HUMAN
MCM3_HUMAN
MCM5_HUMAN
MCM6_HUMAN
MCM7_HUMAN
PCNA_HUMAN
PRI2_HUMAN
RFA1_HUMAN
RFA2_HUMAN
RFC1_HUMAN
RFC2_HUMAN
RFC3_HUMAN
RFC4_HUMAN
RFC5_HUMAN
FACD2_HUMAN
FANCI_HUMAN
MSH2_HUMAN
MSH6_HUMAN
PRKDC_HUMAN
RECQ1_HUMAN
RIF1_HUMAN
SMC3_HUMAN
XRCC5_HUMAN
XRCC6_HUMAN
REPLISOME COMPONENTS
DNA REPAIR PROTEINS
No data available
-
+
B
Input
iPOND
-
Pulse
15' EdU/HU
2h HU
14h HU
Chase
MCM6 (l.e.)
MCM6 (s.e.)
H3
Cdc45
PCNA
Fen1
FANCD2
H3
RFC3
RPA32 (l.e.)
RPA32 (s.e.)
H3
SMC3
H3
SMC1
H3
RAD51
H3

Figure 2.

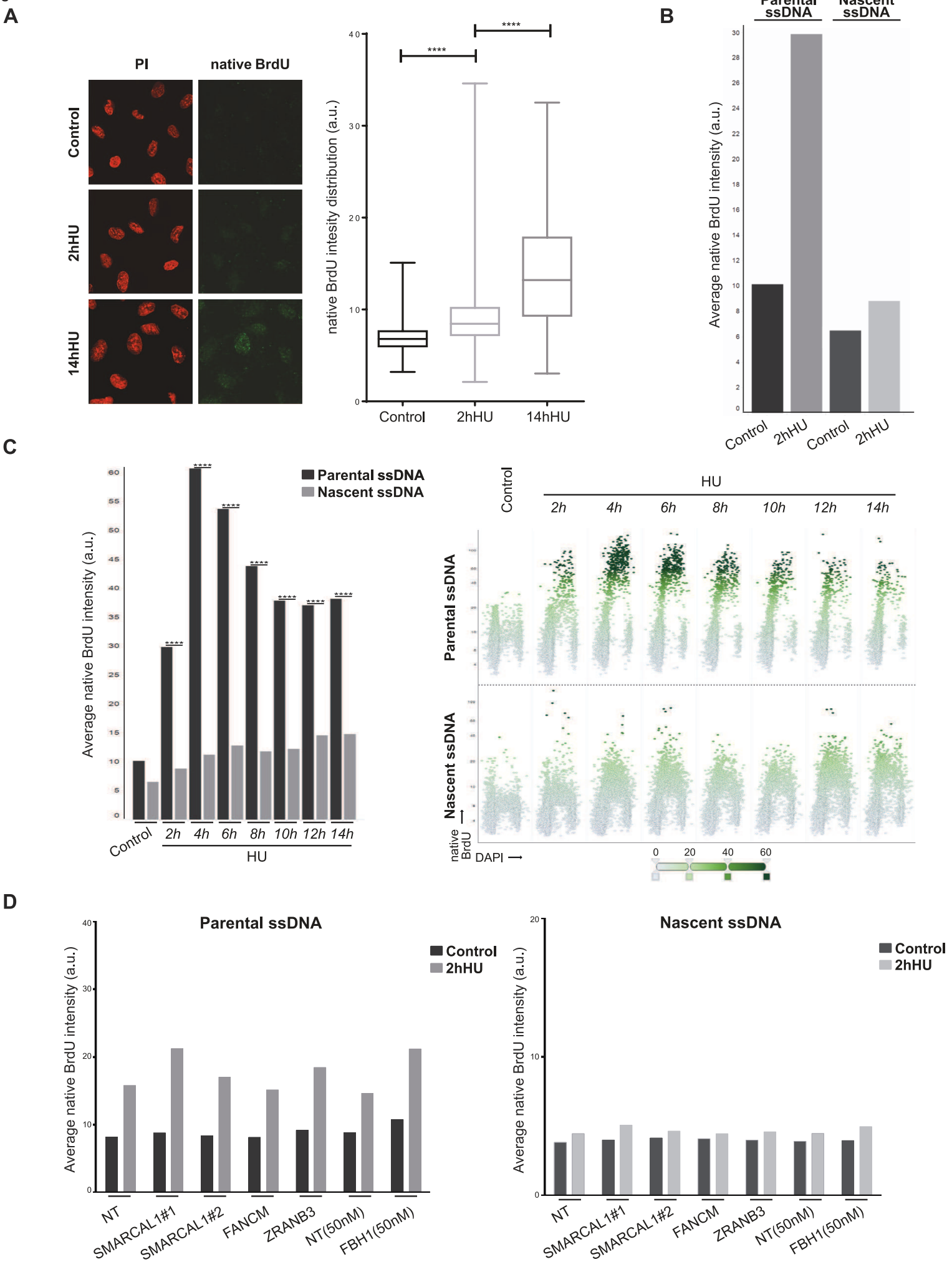
A
PI
native BrdU
Control
2hHU
14hHU
native BrdU intesity distribution (a.u.)
****
****
Control
2hHU
14hHU
B
Parental ssDNA
Nascent ssDNA
Average native BrdU intensity (a.u.)
Control
2hHU
Control
2hHU
C
Parental ssDNA
Nascent ssDNA
Average native BrdU intensity (a.u.)
Control
2h
4h
6h
8h
10h
12h
14h
HU
Control
HU
2h
4h
6h
8h
10h
12h
14h
Parental ssDNA
Nascent ssDNA
native BrdU
DAPI
0
20
40
60
D
Parental ssDNA
Control
2hHU
Average native BrdU intensity (a.u.)
NT
SMARCAL1#1
SMARCAL1#2
FANCM
ZRANB3
NT(50nM)
FBH1(50nM)
Nascent ssDNA
Control
2hHU
Average native BrdU intensity (a.u.)
NT
SMARCAL1#1
SMARCAL1#2
FANCM
ZRANB3
NT(50nM)
FBH1(50nM)

Figure 3.

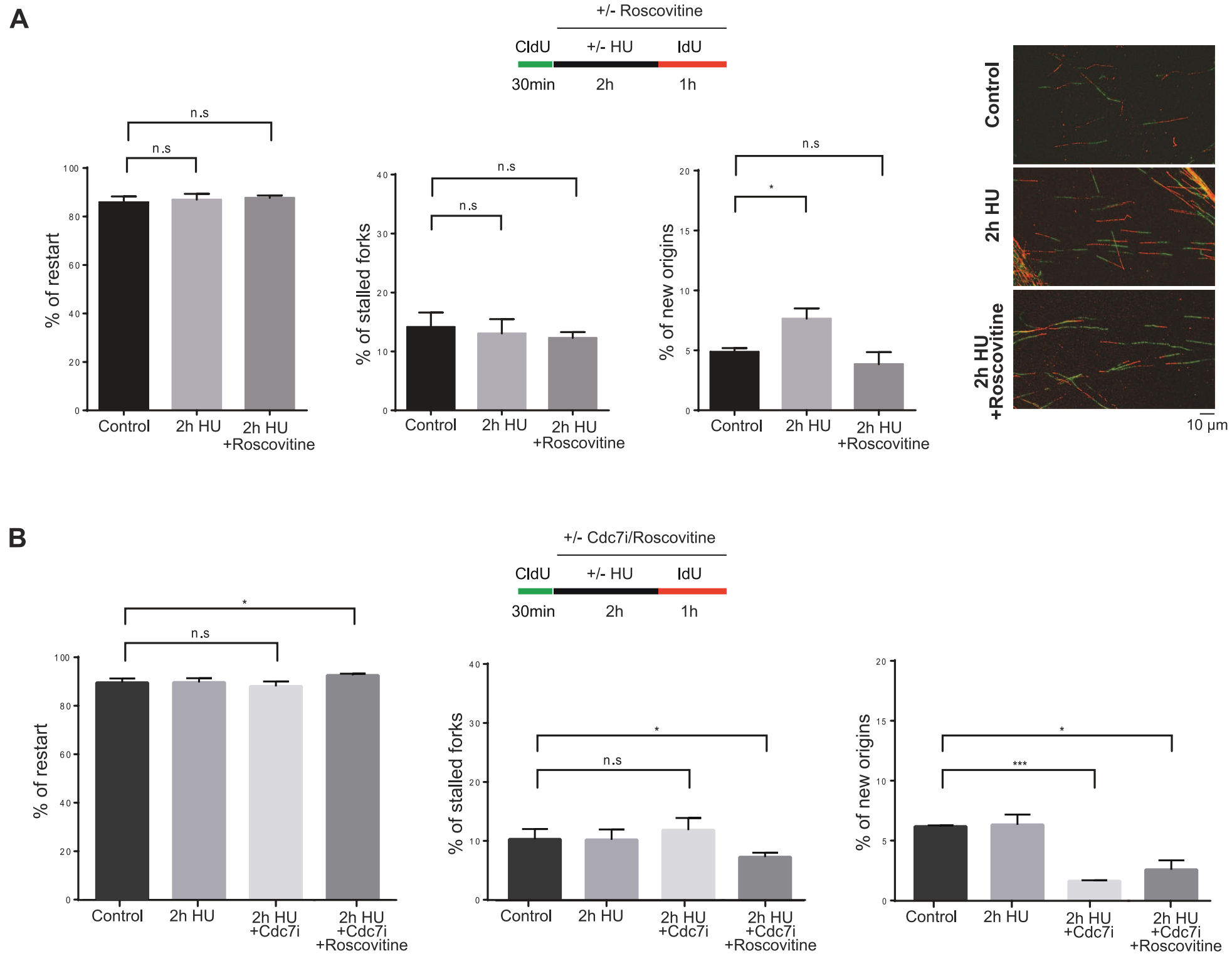
A
+/- Roscovitine
CldU
+/- HU
IdU
30min
2h
1h
% of restart
n.s
n.s
Control
2h HU
2h HU +Roscovitine
% of stalled forks
n.s
n.s
Control
2h HU
2h HU +Roscovitine
% of new origins
n.s
*
Control
2h HU
2h HU +Roscovitine
Control
2h HU
2h HU +Roscovitine
10 µm
B
+/- Cdc7i/Roscovitine
CldU
+/- HU
IdU
30min
2h
1h
% of restart
*
n.s
Control
2h HU
2h HU +Cdc7i
2h HU +Cdc7i +Roscovitine
% of stalled forks
*
n.s
Control
2h HU
2h HU +Cdc7i
2h HU +Cdc7i +Roscovitine
% of new origins
*
***
Control
2h HU
2h HU +Cdc7i
2h HU +Cdc7i +Roscovitine

Figure 4.

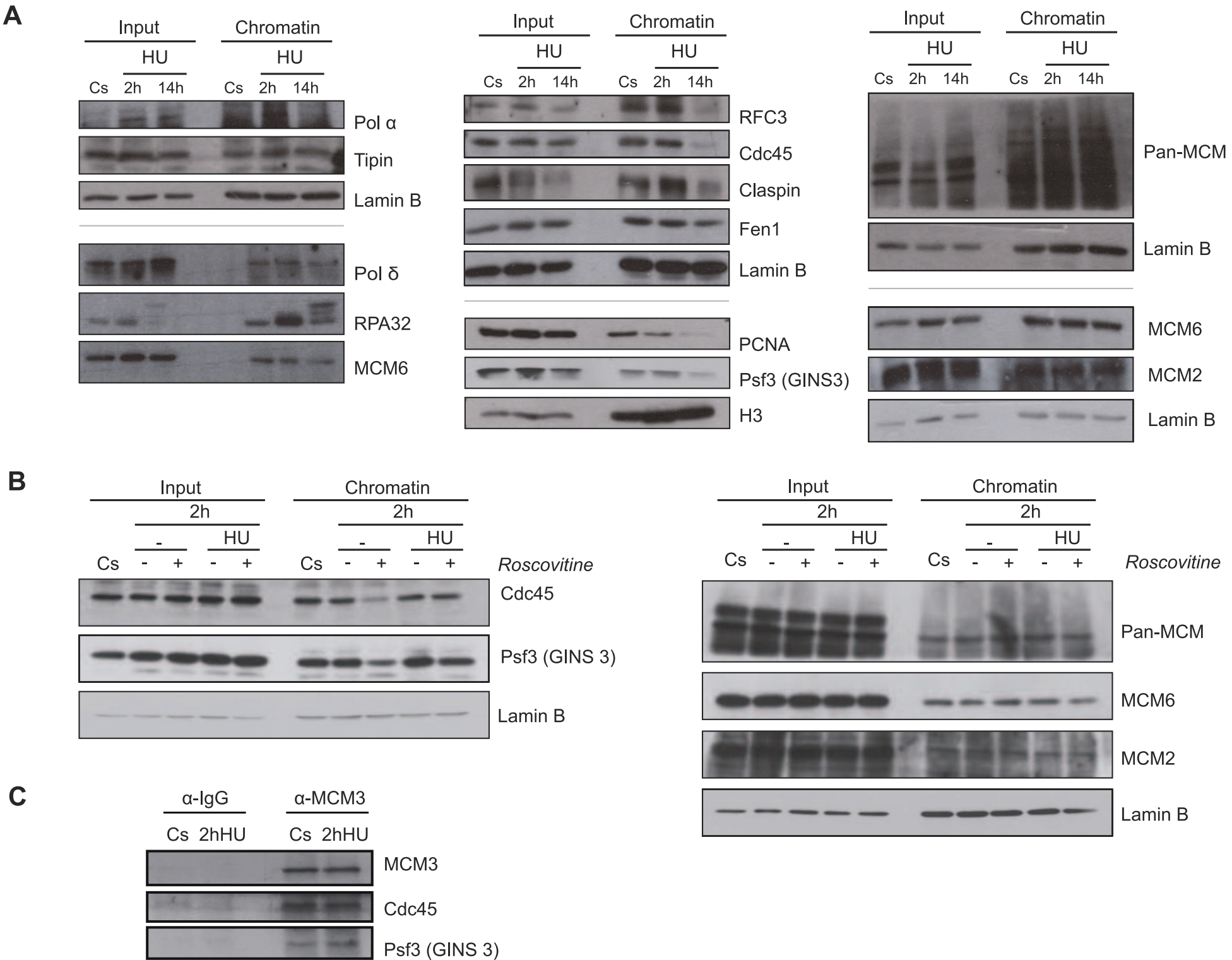
A
Input
Chromatin
HU
Cs 2h 14h
Pol α
Tipin
Lamin B
Pol δ
RPA32
MCM6
RFC3
Cdc45
Claspin
Fen1
PCNA
Psf3 (GINS3)
H3
Pan-MCM
MCM2
B
2h
-
HU
Roscovitine
Psf3 (GINS 3)
C
α-IgG
α-MCM3
Cs 2hHU
MCM3

Figure 5

Figure 5.